HHS Public Access

Author manuscript

Brain Struct Funct. Author manuscript; available in PMC 2018 September 01.

Published in final edited form as:

Brain Struct Funct. 2017 September ; 222(7): 3147–3161. doi:10.1007/s00429-017-1391-5.

Hilar granule cells of the mouse dentate gyrus: effects of age, septotemporal location, strain, and selective deletion of the proapoptotic gene *BAX*

Keria Bermudez-Hernandez[1,2], **Yi-Ling Lu**[2], **Jillian Moretto**[2], **Swati Jain**[2], **John J. LaFrancois**[2], **Aine M. Duffy**[1,2], and **Helen E. Scharfman**[1,2]

[1]New York University Langone Medical Center One Park Avenue New York, NY 10016

[2]The Nathan Kline Institute for Psychiatric Research 140 Old Orangeburg Road Orangeburg, NY 10962

Abstract

The dentate gyrus (DG) principal cells are glutamatergic granule cells (GCs) and they are located in a compact cell layer. However, GCs are also present in the adjacent hilar region, but have been described in only a few studies. Therefore we used the transcription factor prospero homeobox 1 (Prox1) to quantify GCs at postnatal day (PND) 16, 30 and 60 in a common mouse strain, C57BL/6J mice. At PND16, there was a large population of Prox1-immunoreactive (ir) hilar cells, with more in the septal than temporal hippocampus. At PND30 and 60, the size of the hilar Prox1-ir cell population was reduced. Similar numbers of hilar Prox1-expressing cells were observed in PND30 and 60 Swiss Webster mice.

Prox1 is usually considered to be a marker of postmitotic GCs. However, many Prox1-ir hilar cells, especially at PND16, were not double-labeled with NeuN, a marker typically found in mature neurons. Most hilar Prox1-positive cells at PND16 co-expressed doublecortin (DCX) and calretinin, markers of immature GCs. Double-labeling with a marker of actively dividing cells, Ki67, was not detected. These results suggest that, surprisingly, a large population of cells in the hilus at PND16 are immature GCs (Type 2b and Type 3 cells).

We also asked whether hilar Prox1-ir cell numbers are modifiable. To examine this issue we conditionally deleted the proapoptotic gene *BAX* in Nestin-expressing cellss at a time when there are numerous immature GCs in the hilus, PND2-8. When these mice were examined at PND60, the numbers of Prox1-ir hilar cells were significantly increased compared to control mice. However, deletion of *BAX* did not appear to change the proportion that co-expressed NeuN, suggesting that the size of the hilar Prox1-expressing population is modifiable. However, deleting *BAX*, a major developmental disruption, does not appear to change the proportion that ultimately become neurons.

Corresponding author: Keria Bermudez-Hernandez; Current address: New York University Langone Medical Center, Center for Health Informatics & Bioinformatics, 227 East 30th Street, 7th Floor, New York, NY 10016.

Keywords

Prox1; progenitor; programmed cell death; adult neurogenesis; migration; stem cell

INTRODUCTION

The dentate gyrus (DG) is primarily composed of glutamatergic granule cells (GCs) which form a compact cell layer (GC layer). The GCs are organized in the same orientation, with dendrites on one side of the cell body, where they fill the so-called molecular layer, and the axon on the other side of the soma, where the hilar region is located. The hilus lies between the GC layer and area CA3. The GC axons, also called mossy fibers, enter the hilus and then pass into area CA3 where they terminate on pyramidal cells and interneurons (Altman and Das 1965).

Despite the fact that the majority of GCs in normal conditions are located in the GC layer, there are reports of cells that appear to be GCs that are located in the hilus. For example, in Golgi studies, neurons were identified in the hilus that had the morphology of GCs, but were considered to be interneurons (Amaral 1978). GC-like cells were also reported in the hilus in other studies (Marti-Subirana et al. 1986; for review, see Scharfman et al. 2007). In adult rats, hilar neurons with the electrophysiological characteristics of GCs were recorded in hippocampal slices (Scharfman et al. 2003). GCs have also been identified in the CA3 subfield based on both anatomical and electrophysiological criteria (Szabadics et al. 2010). However, few quantitative studies in normal animals have been made, leaving the impression that these hilar GCs or GC-like cells are rare. One study compared saline-treated control rats to pilocarpine-treated adult male rats, where hilar ectopic GCs (hEGCs) are numerous (McCloskey et al. 2006). A substantial number of hilar cells were identified as GCs in the saline-treated controls (McCloskey et al. 2006). Similarly, a study of *Pcmt1*$^{-/-}$ mice showed that wild type (WT) mice and transgenics have hilar GCs, and they were quantified (Farrar et al. 2005).

The purpose of this study was to address the extent that hilar GCs are present in normal mice and address them more quantitatively across the septotemporal axis and by age than prior studies. Notably, the prior study of *Pcmt1*$^{-/-}$ mice examined control mice as well as transgenics, and the background strain was a mixture of C57BL/6J and 129svJae.

After examining C57BL/6J mice, which were chosen because they are commonly used for research, we asked if hilar GCs were also present in Swiss Webster (SW) mice. Examining more than one mouse strain is important because strain differences are common in studies of adult GC neurogenesis (Kempermann et al. 1997; Hayes and Nowakowski 2002; Schauwecker 2006; Kim et al. 2009), the process where adult GCs are generated in postnatal life (Gage et al. 2015). The numbers of GCs in the hilus were studied at three ages: 16, 30 and 60 days after birth (postnatal day or PND16, 30, and 60). These ages were selected because they reflect three developmental stages: 1) a time during development when the DG cell layers have become well defined, but the DG is still not mature (PND16), 2) a time when most aspects of DG circuitry have matured but there is still a high proliferation rate (PND30; Bayer 1982; Rao et al. 2006; Cushman et al. 2012; Ho et al. 2012) and 3) shortly

after puberty when animals are reproductively mature and therefore adults (PND60; Pritchett and Taft 2007).

Prospero homeobox 1 (Prox1) was used as a marker of GCs (Pleasure et al. 2000; Galeeva et al. 2007; Galichet et al. 2008; Steiner et al. 2008; Lavado et al. 2010; Iwano et al. 2012), and the neuronal marker NeuN (Mullen et al. 1992) was used to distinguish immature cells (Prox1+/NeuN−) from mature neurons (Prox1+/NeuN+). We also asked if genetic perturbations could increase hEGCs. A previous study showed a large number of hEGCs in mice with constitutive deletion of the proapoptotic gene *BAX* (Sun et al. 2004; Myers et al. 2013) suggesting that removing a major pathway for programmed cell death would increase the hEGC population. To address this hypothesis, *BAX* was deleted during the first postnatal week, because this is a time when GC proliferation is high (Schlessinger et al. 1975; Martin et al. 2002; Mathews et al. 2010) and the hilus has many Prox1-expressing cells (Altman and Bayer 1990a; b; Pleasure et al. 2000; Li et al. 2009; Lavado et al. 2010; Nicola et al. 2015). Also, the first postnatal weeks are a time when the new GCs undergo substantial programmed cell death (Gould et al. 1991; Dayer et al. 2003; Heine et al. 2004). *BAX* was deleted conditionally in Nestin-expressing cells using NestinCreER^{T2} mice that were crossed with mice that had a floxed (f) *BAX* gene (BAX$^{f/f}$ mice; Sahay et al. 2011), and the outcome was examined using Prox1 and NeuN immunohistochemistry at PND60. Besides asking if the numbers of hilar cells increased we also addressed another question, whether the proportion of hilar GCs that became neurons would be influenced by *BAX* deletion. Our results show that there is a robust population of Prox1-expressing cells in the hilus in C57BL/6J and SW mice, they vary by age, strain and septotemporal position, and their numbers can be increased by *BAX* deletion, although the proportion that become neurons does not.

MATERIALS AND METHODS

General procedures

All experiments were conducted in accordance with the National Institutes of Health (NIH) guidelines and were approved by the Institutional Animal Care and Use Committee (IACUC) of The Nathan Kline Institute. Every effort was made to reduce the numbers of animals used in the study, as well as any pain and discomfort. Reagents were purchased from Sigma-Aldrich (St. Louis, MO) unless stated otherwise.

Animals—C57BL/6J mice (Jackson Laboratories, Bar Harbor, ME) or SW Crl:CRW mice (Charles River Laboratories, Kingston, NY) were used one week after shipment to allow for acclimation, or bred in-house from breeders purchased at these facilities. It is acknowledged that this differences in origins could have affected the results but we have no evidence for it at the present time. To define postnatal age in days, the 24 hours after birth was defined as the first postnatal day or PND1. In the text, “PND16 mice” refers to mice that were PND16, “PND30 mice” were PND31-34, and “PND60 mice” were PND63-66.

The NestinCreER^{T2} Bax$^{f/f}$ (NCBax$^{f/f}$) mouse line was kindly provided by Dr. Amar Sahay and Dr. Rene Hen. The background strain was C57BL6 and Sv129 (Sahay et al. 2011). These mice were created by crossing mice that had *loxP* sites flanking the *BAX* gene

($Bax^{f/f}$) with a NestinCreER^{T2} (NC) mouse line in which tamoxifen-inducible Cre recombinase (CreER^{T2}) is expressed under the control of a rat 5.26 Kb Nestin promoter fragment (Sahay et al. 2011). NC$Bax^{f/f}$ mice (either $NC^{+/-}Bax^{f/f}$ or $NC^{-/-}Bax^{f/f}$, either males or females) and $BAX^{f/f}$ mice (either males or females) were used for breeding. The resultant offspring were either $NC^{+/-}Bax^{f/f}$ or $NC^{-/-}Bax^{f/f}$ and were distinguished by genotyping for Cre recombinase.

After litters were born, lactating females were given 2 mg tamoxifen (0.2 ml of 10 mg/ml dissolved in 10% ethanol in corn oil, i.p.) to delete *BAX* in Nestin-expressing cells as established previously (Sahay et al. 2011). Vehicle was 0.2 ml of 10% ethanol in corn oil. One injection was given daily from PND2 to PND8. Pups were examined at P60 and consisted of four groups: 1) tamoxifen-treated $NC^{+/-}Bax^{f/f}$ mice ($NCBax^{f/f}$); 2) vehicle-treated $NCBax^{f/f}$ mice; 3) tamoxifen-treated $NC^{-/-}Bax^{f/f}$ ($Bax^{f/f}$) mice; and 4) vehicle-treated $Bax^{f/f}$ mice.

Mice were housed in standard mouse cages with corncob bedding. They had access to water and food (Purina 5001 chow; W.F. Fisher, Somerville, NJ) *ad libitum*, and were maintained on a 12 hour light/dark cycle.

Perfusion and tissue preparation—Mice were deeply anesthetized by inhalation of isoflurane followed by an intraperitional (i.p.) injection of urethane (2.5 g/kg) dissolved in 0.1 M phosphate buffer (PB, pH 7.4). Mice were transcardially perfused following a midline incision to open the pericardial cavity and after clipping the left atria. Using a peristaltic pump (Minipuls 1; Gilson, Middleton, WI), 15 ml of 0.9% NaCl was infused within ~3 minutes followed by >15 ml of 4% paraformaldehyde (PFA; Electron Microscopy Supplies, Hatfield, PA) in 0.1 M PB at the same rate. Brains were removed and post-fixed in 4% PFA for at least 24 hours.

After fixation, brains were sectioned in two ways. The first method allowed sectioning of the hippocampus throughout the septotemporal axis in a plane similar to transverse sections. This approach allowed one to sample the hilus with an orientation that made hilar borders easily defined throughout the septotemporal axis. First, hemispheres were separated at the midline by a razor blade and the hippocampus was isolated from one hemisphere by inserting a curved spatula between the alveus and corpus callosum at the medial surface. The isolated hippocampus was “rolled” away from the overlying cortex and cut off from adjacent parts of the brain. It was immersed in warm (38–40°C) 4% agar (Fisher Chemical Co, Fair Lawn, NJ) dissolved in distilled H_2O, allowed to cool to room temperature, and then hardened by immersion in 2% PFA for at least 2 hours at 4°C. Then the agar block was glued with cyanoacrylate (Krazy glue, Westerville, OH) to a vibratome stage and serially sectioned (50 μm-thick sections; TPI 3000, Vibratome Co, St. Louis, MO) perpendicular to the long axis of the hippocampus (Figure 1).

In addition to transverse sections from the isolated hippocampus, mice were perfused and the brain was postfixed in 4% PFA for at least 1 day, and then sectioned. These hippocampi were cut in common planes of section, the coronal or horizontal plane. Data using the ‘isolated’ hippocampus were compared to data from sections made in the coronal and

horizontal plane to determine if results were independent of technical approach. Using one hemisphere from perfused mice, sections were cut in the coronal plane. For theother hemisphere, sections were cut in the horizontal plane. Coronal sections were cut starting at the septal pole and ending at the point along the rostral-caudal axis when the curvature of the hippocampus makes hilar borders difficult to interpret (4.0 mm posterior to Bregma; Paxinos and Watson 2007). Four-five sections were selected from the center of this region (~2.0–3.0 posterior to Bregma) with 150 μm between sections. Horizontal sections were cut from the second hemisphere, starting at the extreme temporal pole (~2.5 from the interaural line; Paxinos and Watson 2007) and ending in the dorsal part of the hippocampus when boundaries of the hilus became hard to discern (~6.0 mm from the interaural line; Paxinos and Watson 2007). Horizontal sections (4–5) were selected from the center of this region, with a relatively large intersection interval (300 μm) because the region spanned a large distance (3.0–5.0 mm from the interaural line).

Immunohistochemistry—Free-floating sections were processed as follows. First, sections were washed (3 × 5 minutes) in 0.1 M Tris buffer (pH 7.4), incubated in 1% hydrogen peroxide in 0.1 M Tris buffer for 30 seconds and washed in 0.1M Tris buffer (3 × 5 minutes). Sections were incubated in blocking serum (10% normal goat serum; Vector Laboratories, Burlingame, CA) in 0.1 M Tris buffer for 30 minutes followed by a 10 minute-long wash in 0.1 M Tris buffer with 0.25%Triton X-100 (referred to as Tris A) and a 10 minute-long wash of 0.1 M Tris buffer with 0.25% Triton X-100 and 0.005% bovine serum albumin (referred to as Tris B). Next, sections were incubated in primary antibody for 24 hours on a rotator at room temperature. Specificity of antibodies is described in Supplemental Table 1. On the next day, primary antibody (rabbit polyclonal anti-Prox1, 1:10,000; catalog number 11-002; AngioBio, Del Mar, CA) was diluted in Tris B, sections were washed in Tris A for 10 minutes and Tris B for 10 minutes, followed by a 30 minute-long incubation of secondary antibody (biotinylated anti-rabbit IgG made in goat; 1:400; Vector) diluted in Tris B. Subsequently, sections were washed in Tris A for 10 minutes and Tris B for 10 minutes, followed by 1 hour incubation in avidin-biotin horseradish peroxidase complex (ABC; Vectastain Elite ABC Kit; Vector) diluted in Tris B. Sections were washed with 0.1 M Tris buffer (3 × 5 minutes) and reacted in 0.22% 3, 3'-diaminobenzidine (DAB), 0.2% ammonium chloride, 0.1% glucose oxidase, and 5 mM $NiCl_2$ in 0.1 M Tris buffer. Experimental and control groups were processed together. Sections were processed in the same order from one step to the next, so that the times that sections were incubated in reagents were similar. Sections were washed in 0.1 M Tris buffer (3 × 5 minutes), mounted on 0.1% gelatin-coated slides, dehydrated in a graded series of alcohols (70%, 3 minutes; 95%, 3 minutes; 100%, 2 × 5 minutes), incubated in Xylene (2 × 5 minutes), and coverslipped with Permount (Fisher).

For double-labeling of DAB-labeled Prox1-ir cells with NeuN, incubation with DAB was followed by 2 × 5 minutes washes in 0.1 M Tris buffer and then 30 minutes incubation with 5% normal horse serum (Vector) made in Tris B. Then sections were washed in Tris A for 10 minutes and Tris B for 10 min, followed by incubation in primary antibody to NeuN (mouse anti-NeuN; 1:5,000; catalog number MAB 377, Millipore, Temecula, CA) while rotating for 24 hours at room temperature. On the next day, sections were washed with Tris A for 10

minutes and Tris B for 10 minutes, followed by incubation with secondary antibody (biotinylated anti-mouse IgG made in horse; 1:400 in Tris B; Vector) for 30 minutes. Subsequently, sections were washed in Tris A for 10 minutes and Tris B for 10 minutes, followed by incubation in ABC in Tris B. Then sections were reacted with NovaRed (Vector) according to the manufacturer's instructions. The NovaRed solution included the following (per 5 ml of distilled H_20): 3 drops of Reagent 1, 3 drops of Reagent 2, 2 drops of Reagent 3, and 2 drops of hydrogen peroxide. The reaction was stopped with washes in 0.1 M Tris buffer (2 × 5 minutes). Sections were mounted on 0.1% gelatin-coated slides, dehydrated and coverslipped as described above.

Sections were photographed with a brightfield microscope (BX51, Olympus of America, Center Valley, PA) and digital camera (RET 2000R-F-CLR-12, Q Imaging, Surrey, BC, Canada).

Immunofluorescence—Free floating sections were washed (2 × 5 minutes) in 0.1 M PB, incubated in blocking serum for 1 hour (10% donkey serum, 0.025% Triton X-100 and 0.005% bovine serum albumin in 0.1 M PB), washed (3 × 5 minutes) in 0.1 M PB and incubated overnight in 4°C with a primary antibody solution diluted in 1% donkey serum and 0.35% Triton X-100. The next day, sections were washed in 0.1 M PB (3 × 5 minutes), followed by a 2 hour-long incubation in a solution containing secondary antibodies diluted in 0.1 M PB, 1% donkey serum and 0.25% Triton-X-100.

For Prox1, the primary antibody was a polyclonal antibody made in goat (1:1,000; R&D systems; catalogue # AF2727; Minneapolis, MN) instead of rabbit because double-labeling was conducted using antibodies made in rabbit. Notably, we did not detect differences in results with the two antibodies. Nevertheless, brightfield studies (rabbit antibody) were not directly compared to immunofluorescence (goat antibody) in the Results. For calretinin, a rabbit polyclonal primary antibody was used (1:5,000; catalogue # AB5054, Millipore, Temecula, CA). For DCX, a goat polyclonal was the primary antibody (1:2,000; Santa Cruz); for Ki67, a rabbit polyclonal antibody was the primary antibody (1:500; catalogue # VPK451, Vector). As for antibodies used for brightfield microscopy, specificity of antibodies is described in Supplemental Table 1.

For Prox1, the secondary antibody was donkey anti-goat (Alexa fluor 488; 1:500; catalogue # A11055; Life Technologies, Grand Island, NY); for calretinin and Ki67, a donkey anti-rabbit secondary antibody was used (Alexa fluor 546; 1:500; catalogue # A10040; Life Technologies, Grand Island, NY); for DCX, a donkey anti-goat secondary antibody was used (Alexa fluor 568; 1:500; catalog # 11057; Life Technologies).

Sections were mounted on 0.1% gelatin-coated slides, and coverslipped with Vectamount (Vector). Sections were viewed with a confocal microscope (LSM 510 Meta; Carl Zeiss Microimaging, Thornwood, NY).

Quantification of Prox1-ir cells—Pilot studies showed that Prox1-ir cells were rare in some animals, i.e. older control mice. In addition, Prox1-ir cells clustered near the SGZ in some cases, i.e. tamoxifen-treated NCBax$^{f/f}$ mice. This meant that the hilar distribution of

Prox1-ir cells was not always random. Therefore, the optical fractionator was not employed; instead a method was used that counted all hilar Prox1-ir cells. Three criteria were used to define a hilar Prox1-ir cell: 1) the hilar cell had sufficient Prox1-ir to reach a threshold equal to the average level of Prox1-ir of GCs in the adjacent GC layer, 2) the hilar Prox1-ir cell had a cell body size that fell into the range of cell body sizes measured for GCs in the adjacent GC layer. All hilar Prox-ir cells were complete, i.e. not cut at the surfaces of the section. Computerized methods for assessing cell numbers, and additional details, are described in Supplemental Methods. It should be noted that we report "hilar" GC estimates because the word "ectopic" denotes abnormal location, and cells in the SGZ are not very far from the normal location.

Density was calculated either for a single septotemporal level or the entire hippocampus. To calculate density for a single level, the estimated number of cells of a given section was divided by the area of the hilus in that section. To estimate the total number of cells per hippocampus, the estimated number of cells for each section was summed. This was only done for analysis of the isolated hippocampus where the entire septotemporal axis was assessed. The total number of cells was divided by the reciprocal of the section sampling fraction (ssf): $N=\frac{1}{ssf}\times\sum n$. One of every 5 sections (250 μm apart) were used for assessment of cells per hippocampus based on pilot studies showing that septotemporal differences would be probe with this frequency of sampling. Sampling of the hilus included the main region of the hippocampus where both of the DG blades are present; the extreme poles of the hippocampus were not sampled because at these locations it is difficult to define the hilus. Hilar area was defined as the region surrounded by the GC layer and a line between the lateral tips of the GC layer. A figure showing this region schematically is provided in the Supplemental Methods. To estimate hilar volume per hippocampus, the following formula was used where T was the section thickness (50 μm) and A the hilar area: $V=1/ssf\times T\times\Sigma A$.

In some cases, hilar Prox1-ir cells overlapped, although not many (typically 2–3 when viewed at high power). To quantify cell number in this situation, the area of the overlapping cells was measured and divided by the mean GC cell body area. The approach was validated by comparing the results to manual counts and showing that the differences were not significant. The method and comparisons are shown in the Supplemental Methods.

Quantification of double-labeled cells—Double-labeled cells were counted manually. A cell was defined as double-labeled if the nucleus and cytoplasm were brought into focus simultaneously at 80X magnification, i.e., they were located in the same optical section. For brightfield microscopy focusing was done manually; for immunofluorescence it was done using multiple thin (1–1.5 μm) optical sections and 3D rotation.

Statistics—Data are expressed as mean ± SEM. The p criterion was 0.05. Linear regression, ANCOVA, Student's t-tests, and ANOVAs were performed in GraphPad Prism 6 (La Jolla, CA). After ANOVAs, a Tukey-Kramer post-hoc test was performed to compare individual groups. Interactions between factors are only reported when they were significant.

RESULTS

I. Prox1-ir hilar cells in normal mice

A. Prox-ir hilar cells are a significant fraction of hilar cells and decrease with age—The first goal was to determine whether Prox1 -ir cells formed a robust population in the hilus of normal C57BL/J mice. First, Prox1-ir cells were clearly present in the hilar region at all three ages (Figure 1C–D). A one-way ANOVA showed that there was a significant effect of age on hilar Prox1-ir cell density [$F(2,11)351.20$; $p < 0.0001$] with the greater density at P16 than P30 ($p < 0.05$) and P60 ($p < 0.05$).

The differences in hilar Prox1-ir density with age could have been caused by differences in cell numbers or hilar area, so these parameters were also quantified. As shown in Supplemental Figure 1, hilar Prox1-ir numbers were similar to density in that they decreased with age [one-way ANOVA; $F(2,11)$ 96.38; $p < 0.0001$], with Prox1-ir cells greatest at PND16 (post-hoc tests, $p < 0.05$; Supplemental Figure 1A). A similar result was also obtained by linear regression; there was an inverse relationship between hilar Prox1-ir cell number and age (Linear regression, $r^2 = 0.855$, $p < 0.0001$). There were no significant differences in hilar volume at the different ages [one-way ANOVA; $F (2, 11)$ 2.86; $p = 0.100$; Supplemental Figure 1B]. In summary, the results showed that at PND16, there are many hilar Prox1-ir cells. After PND16, hilar Prox1-ir cell density and numbers of Prox1-ir cells decrease with age, while hilar volume does not.

B. The proportion of hilar Prox1-ir cells that are mature neurons increases with age—To determine if Prox1-ir cells were mature neurons, we determined if cells expressing Prox1 were labeled using an antibody to the neuronal marker NeuN. We used septal sections from isolated hippocampi (n=3 mice, 2 sections/mouse) because this was where the highest hilar Prox1-ir cell density was found.

As shown in Figure 2A–B, there was a main effect of age on the percentage of hilar Prox1-ir cells that co-expressed NeuN, with over 10-fold more mature neurons at PND60 than PND16 (4.4 ± 1.3% at PND16 vs. 58.1 ± 8.3% at PND60; Figure 2B). Furthermore, there was an inverse relationship between the percentage of hilar Prox1+/NeuN+ double-labeled cells and age (Linear regression; $r^2 = 0.838$, $p = 0.001$). These data suggested that the majority of Prox1-ir cells at PND16 are at a relatively immature stage of development, and more Prox1-ir cells become mature neurons with time.

C. A robust population of Prox1-ir cells exists in PND16 mice—The results shown in Figures 1–2 suggest that a large population of hilar cells express Prox1 at PND16. Because many of these cells did not coexpress NeuN, we determined their phenotype using markers that would be expressed before the NeuN stage. Ki67 was used to label cells that are actively dividing (Gerdes et al. 1991 ; Key et al. 1992; Key et al. 1993), DCX was used to label cells that had already committed to a neuronal fate but were still immature (Brandt et al. 2003; Brown et al. 2003; von Bohlen Und Halbach 2007), and calretinin was used because it labels a transient stage in development of young GCs (Cowan et al. 1980; Brandt et al. 2003; Kempermann et al. 2004; Lazarov et al. 2010; Nicola et al. 2015; Zhang and Jiao 2015).

We found that many Prox1+ cells at PND16 expressed calretinin (Figure 3, Supplemental Figure 2). In 3 mice (2 sections/mouse), a total of 225 Prox1+ cells were examined. The mean percentage of Prox1 +/calretinin+ double-labeled cells was 81.8 ± 5.2%. Therefore, the majority of hilar Prox1-ir cells in PND16 C57BL/6J mice were immature GCs.

We also found that many Prox1 + cells co-expressed DCX (Figure 3, Supplemental Figure 3). Over 200 cells were examined that expressed Prox1 and the mean percentage of Prox1 + cells that were also DCX+ was 60.9 ± 9.9 % (n=3 mice, 2 sections/mouse). There was no statistical difference between the percentages of Prox1 +/calretinin+ (81.8 ± 5.2%) and Prox1+/DCX+ (60.9 ± 9.9%) cells (Student's t-test, $p = 0.139$). It is important to note that co-expression was technically more difficult to interpret for DCX than calretinin because DCX labeled the cytoplasm of the soma weakly; instead, DCX labeled processes mostly (Figure 3; Supplemental Figure 5). Z-stacks of many optical sections had to be used to be sure of double-labeling. In 8.4 ± 1.3 % (range, 5.8–10.8%) of Prox1 -ir cells, the double-labeling was not clear so it was not defined as double-labeled. Therefore, the percentage of double-labeled cells (Prox1 + DCX+) could be an underestimate.

There was no evidence that Prox1-ir cells were actively dividing because no double-labeling was detected using Ki67 (Figure 3). Because no cells were detected in the initial analysis, we examined more (a total of 6–7 sections were sampled along the entire septotemporal axis, 1 section for every 10, n=4 mice) to be sure of the negative result, and it was confirmed. In summary, a large population of immature GCs is present in the C57BL/6J mouse at PND16 and they are mostly immature GCs.

D. Effect of septotemporal location on hilar Prox1-ir cells—During development, the temporal pole of the DG matures first (Schlessinger et al. 1975). In adulthood, neurogenesis in C57BL6 mice is greater in the septal pole compared to the temporal DG (Choi et al. 2007; Snyder et al. 2009; Jinno 2011a). For these reasons we asked if there was a septotemporal gradient in hilar Prox1-ir cells. We used isolated hippocampi from C57BL6 mice (PND16, n=4; PND30, n=5; PND60, n=5). As shown in Figure 4A, septal hilar Prox1-ir cell density was high and gradually decreased as the section location approached the temporal pole (Figure 4A). Comparison of the slopes of the plots in Figure 4A showed that there were significant differences [ANCOVA; $F(2, 173)$ 15.29; $p < 0.0001$]. A two-way RMANOVA was significant, with main effects of age and septotemporal level, as well as an interaction of factors (Figure 4A). Greater cell density in septal DG was also observed using sections from hemispheres rather than isolated hippocampi (Supplemental Figure 4). A two-way ANOVA showed a significant effect of septotemporal location [$F(1, 12)$ 23.26; $p = 0.0004$] and age [$F(2, 12)$ 88.57; $p < 0.0001$; Supplemental Figure 6].

The differences in density along the septotemporal axis could have been influenced by a septotemporal difference in hilar size. Therefore, cell numbers and volume of the hilus were plotted for each section from the isolated hippocampi (Supplemental Figure 5). Prox1-ir cell numbers were greater in septal compared to temporal hippocampus (Supplemental Figure 5A). Hilar area increased from septal to temporal DG, and the data were almost superimposable for all three ages (Supplemental Figure 5B). Therefore, hilar area could have influenced the relationship of hilar Prox1-ir cell density to septotemporal location, but was

not the only factor, because the septotemporal gradient was evident in cell numbers without taking the hilar area into account at all.

These results suggest that more hilar Prox1-ir cells are located in septal compared with the temporal hippocampus at PND16. In addition, the differences in hilar Prox1-ir cell density between septal and temporal hippocampus decrease with age.

E. Strain differences in hilar Prox1-ir cells—Many aspects of the DG vary among mouse strains; for example, adult neurogenesis varies in the rate of proliferation and survival (Kempermann et al. 1997; Hayes and Nowakowski 2002; Schauwecker 2006; Kim et al. 2009). Therefore, we asked if C57BL/6J mice had a different density of hilar Prox1-ir cells than another strain. Because C57BL/6J mice are an inbred strain, we selected an outbred strain (SW) for comparison. Analyses were confined to PND30 and PND60 and isolated hippocampi (Figure 4B). There was no effect of strain on hilar Prox1-ir cell density by two-way ANOVA [F(1,16)2.13; $p = 0.164$] but there was an effect of age [F1, 16) 21.42; $p = 0.0003$]. PND30 mice exhibited significantly greater hilar Prox1-ir cell density in both C57BL/6J and SW mice (post-hoc tests, $p < 0.05$; Figure 4B).

When hilar Prox1-ir cell distribution was compared along the septotemporal axis, linear regression showed that density decreased from the septal to temporal pole in C57BL/6J mice at each age (PND30: $r^2 = 0.463$, $p < 0.0001$; PND60: $r^2 = 0.416$, $p < 0.0001$; Figure 4C). In SW mice, the linear regression did not show a significant relationship between hilar Prox1-ir cell density and septotemporal level at either age (PND30: $r^2 = 0.038$, $p = 0.116$; PND60: $r^2 = 0.032$, $p = 0.145$; Figure 4C). When data from SW mice were analyzed by two-way RMANOVA (factors: age and septotemporal location), there was no effect of septotemporal level [F (11, 88) 0.96; $p = 0.488$; Figure 4C]. These data suggested that septotemporal differences were present in C57BL/6J mice but not SW mice.

II. Effects of removal of BAX in Nestin-expressing cells from PND2-8 on hilar Prox1-ir cells

The number of adult-born GCs derived can be increased by interfering with apoptosis, which occurs after deleting *BAX* (Sun et al. 2004; Sahay et al. 2011; Myers et al. 2013). To test this hypothesis we used isolated hippocampi from $NCBax^{f/f}$ mice which were administered tamoxifen or vehicle at PND2-8 as described in the Methods. In addition, we examined mice with only the floxed *BAX* gene (tamoxifen or vehicle-injected $Bax^{f/f}$). As shown in Figure 5A–C, tamoxifen-treated $NCBax^{f/f}$ mice had the most hilar Prox1-ir cells of all four experimental groups [one way-ANOVA; F (3, 8) 23.50; $p = 0.0003$ followed by post-hoc tests, $p < 0.05$]. $NCBax^{f/f}$ mice treated with tamoxifen had ~3.2 times greater density of hilar Prox1-ir cells compared to controls (Figure 5C). Hilar volume was similar in each group [F (3, 8) 3.07; $p = 0.091$; Supplemental Figure 6]. These results, which were obtained at PND60, were similar at PND 30 (Supplemental Figure 7).

Since hilar Prox1-ir cell density was influenced by septotemporal position in C57BL/6J mice, we asked whether hilar Prox1-ir cell density varied along the septotemporal axis after removal of *BAX*. All groups of mice showed a decline in Prox1-ir cell density at temporal locations (Linear regression: tamoxifen-treated $NCBax^{f/f}$: $r^2 = 0.175$, $p = 0.007$; vehicle-treated $Bax^{f/f}$: $r^2 = 0.151$, $p = 0.011$; tamoxifen-treated $Bax^{f/f}$: $r^2 = 0.231$, $p = 0.002$; vehicle-

treated NCBax$^{f/f}$: r^2 = 0.122, p = 0.030; Figure 5D). Taken together, the results suggest that *BAX* removal during the first postnatal week in Nestin-expressing cells leads to increased hilar Prox1-ir cell density compared to controls. The data also suggest that the septotemporal differences were maintained after *BAX* deletion.

To determine if *BAX* deletion influenced the extent that hilar Prox1-ir cells co-expressed NeuN, double-labeling for Prox1 and NeuN was conducted (Figure 5E). Since hilar Prox1-ir cell density was not significantly different among the vehicle-treated NCBax$^{f/f}$ and Bax$^{f/f}$ mice [one-way ANOVA, F (2, 6) 1.721; p = 0.257], they were pooled. In 3 tamoxifen-treated NCBax$^{f/f}$ and 3 vehicle-treated control mice, 2 sections were selected from the middle of the septal region (3.5–3.6 mm posterior to Bregma; Paxinos and Watson, 2007) for each mouse and the averages were compared. Tamoxifen-treated NCBax$^{f/f}$ mice had ~ 4 times more Prox1-ir cells that co-expressed NeuN compared to vehicle-treated controls (tamoxifen-treated NCBax$^{f/f}$: 61.7± 9.9%; controls: 14.0 ± 1.2%; Figure 5E1). However, the percentage of hilar Prox1-ir cells that co-expressed NeuN was not significantly different from controls (tamoxifen-treated NCBax$^{f/f}$: 89.0 ± 1.7%; controls: 91.3 ± 2.0%; Figure 5E2). The results suggest that *BAX* deletion increases Prox1-ir cell numbers in the hilus, but remarkably, the proportion that are NeuN+ at PND60 does not appear to change. Therefore, the regulation of the number of hilar Prox1-ir cells that survive and become hilar GCs is independent of the size of the population – if increased, more neurons do not necessarily develop from the larger pool of immature cells. The results suggest that *BAX* can regulate the survival of Nestin-expressing cells but other factors control the fate choice (i.e., maturation into neurons).

DISCUSSION

I. Prox1-ir cells are a subpopulation of hilar cells

A. PND16—The results showed that Prox1-ir cells are a robust subset of hilar cells in the normal C57BL/6J and SW mouse, especially at PND16. These data are surprising because hilar GCs are only considered to be substantial in the first week of life. Thus, prior studies have described a robust population of hilar Prox1-ir cells reflecting the tertiary matrix stage of development during the first 7–10 days of postnatal life of rats and mice (Pleasure et al. 2000; Li et al. 2009; Lavado et al. 2010; Nicola et al. 2015). At PND 0 (Nicola et al. 2015) and PND7 (Li et al. 2009), these cells densely populate the hilus, but by PND10 (Li and Pleasure 2007) or PND14 (Nicola et al. 2015) most Prox1-ir appears to have shifted to the GC layer and the tertiary matrix stage is ending (Li and Pleasure 2007; Nicola et al. 2015). In the rat, hilar Prox1-ir is rare at PND19 (Pleasure et al. 2000). Although it is hard to compare rat and mouse, from these studies one might expect few hilar Prox-1 ir cells would exist at PND16. However our results suggest that a surprising number are present, especially in the septal hippocampus of C57BL/6J mice.

Of the Prox1-ir cell population in the hilus at PND16, only a small percentage were double-labeled with NeuN. Instead, most hilar Prox1-expressing cells double-labeled with DCX and calretinin, suggesting that the majority were immature GCs. Consistent with that view, Prox1-labeled cells in PND16 mice did not double-label with Ki67. Our results are consistent with studies in rats showing many cells (labeled by retrovirus at P5) are GCs at

early stages of development and they mature and migrate to the GC layer at least until PND12, the last age that was studied (Namba et al. 2005).

One might expect that all immature GCs would express NeuN because in some publications it is reported that NeuN expression develops at the same time as calretinin (Attardo et al. 2010) or earlier (Zhang and Jiao 2015). However, there is variability in the literature with respect to the relative timing of Prox1, DCX, calretinin and NeuN expression. Some of the variability is due to the fact that the expression patterns can depend on when the GC is born — early in life, or in adulthood (Nicola et al. 2015; Zhang and Jiao 2015). For example, DCX has a broad expression pattern in early postnatal life compared to adulthood (Nicola et al. 2015). Our data are consistent with the view that Prox1 expression can occur when DCX and calretinin are present, but NeuN expression has yet to develop (Cowan et al. 1980; Lazarov et al. 2010).

In summary, our results suggest that there are more hilar Prox1-expressing cells at PND16 than previously identified in the mouse DG, at least in C57BL/6J mice. Instead of rare hilar cells that express Prox1 after P10, there are many cells. After PND16 there is a large reduction, but cells are still present as late as PND60. This suggests that the tertiary matrix decays at a slower rate than previously believed.

These conclusions are important for research studies that use mice at PND16 or a similar age. It is important to recognize at these ages there are still many immature GCs in the hilus. Experimental procedures in these young mice may perturb the development of those cells, and therefore the development of the DG.

B. Relative numbers of Prox1-ir cells at PND30 and 60—For density, there were 254 ± 8 cells/mm^2 in C57BL/6J mouse at PND30 and 145 ± 15 cells/mm^2 at PND60. Regarding numbers of cells, there were 1,361 ± 40 cells/hippocampus at PND30, and at PND60 there were 864 ± 91 cells/hippocampus (Supplemental Figure 1). How does this population size compare to other studies of ectopic GCs? The values are hard to compare because different methods were used for tissue processing and quantification, but the numbers of Prox1-ir cells in the adult rat hilus and the adult C57BL/6 hilus appear to be in the same range; adult rat hilar GCs ranged from 500-2,000/hippocampus; these rats were saline-treated controls that were compared to pilocarpine-treated rats that developed epilepsy (McCloskey et al. 2006). For mice, studies of the controls for *Pcmt1*$^{-/-}$ mice (background: C57BL/6 -129svJae) showed a larger number of Prox1-expressing hilar cells, 5,586 per hippocampus (Farrar et al. 2005).

How does the size of the hilar Prox1-ir population compare to other subtypes of cells in the hilus? If one confines the comparison to hilar cells in adult C57BL/6J mice, there is one study where hilar mossy cells, the largest hilar cell population, were quantified, and there were 3,739 ± 313 cells/hippocampus (Volz et al. 2011). These numbers should be compared to the adult mice with caution because the method to quantify mossy cells used GluR2/3 as a marker, and GluR2/3 is expressed in all glutamatergic neurons (both mossy cells and hilar GCs). Nevertheless, the data suggest that hilar Prox1-ir cells in the adult mouse are a robust subset of hilar cells.

C. Decline in hilar Prox1-ir cells between PND 30 and 60—We found a significant decline in hilar Prox1-ir cell density from PND30 to 60. This is surprising because most aspects of the DG circuitry have matured by PND30. However, there are additional changes to GC axons, the mossy fibers, after this age and they have been attributed to final stages of maturation (Amaral and Dent 1981). If GCs are born in adulthood, the axon matures up to 8 weeks after birth (Faulkner et al. 2008). There also is a decline in proliferation between PND30 and PND60 in mice (He and Crews 2007; Cushman et al. 2012) and rats (Bayer 1982; Bayer et al. 1982; Seki and Arai 1995; Cowen et al. 2008). Consistent with these studies, we found that the subset of hilar Prox1-ir cells that are mature GCs (i.e., they express NeuN) increases between PND30 and PND60, suggesting a preferential increase in mature GCs. These changes may be related to puberty, which begins at approximately PND30 in the rodent, and ends at approximately PND50 (Pritchett and Taft 2007).

D. Septotemporal differences—The results showed that there is a septotemporal distribution in hilar Prox1-ir cell density in C57BL/6J mice, and that the septal DG has greater hilar Prox1-ir cell density compared with the temporal DG. The results are consistent with the higher GC proliferation rate in the septal compared to temporal DG in the adult (Ferland et al. 2002) and the evidence of more adult-born GCs in the septal compared with temporal adult DG (Jinno 2011b; a).

This result is also consistent with the slower development of the septal hippocampus compared to the temporal hippocampus (Schlessinger et al. 1975) and the observation that most hilar Prox1-ir cells at PND16 are lost by PND 30, presumably due to apoptosis that occurs during development. Thus, the septal hippocampus may still be developing at PND16 and have many hilar Prox1-ir cells because “pruning” by apoptosis is not yet over. In contrast, the temporal hippocampus may be more mature at PND16, with fewer hilar Prox1-ir cells because pruning of this population is almost over.

E. Hilar Prox1-ir cells in the adult mouse could be a source of stem cells—Although most of the hilar Prox1-ir cells express NeuN at PND60, some do not and could therefore be cells that are still immature. In embryonic life, Prox1 expression occurs in neural progenitors and postmitotic cells (Oliver et al. 1993; Li et al. 2009; Nicola et al. 2015), and in adulthood Prox1 expression occurs in intermediate progenitor cells (Type 2 and 3 stem cells) and then continues to be expressed as the cell becomes a mature GC (Oliver et al. 1993; Galeeva et al. 2007; Urban and Guillemot 2014; Nicola et al. 2015). Based on the idea that Prox1 can be expressed in Type 2b and 3 cells, and these cells have the capacity to divide, it is interesting to consider the idea that the hilus is a site of proliferation in adulthood, not only the SGZ. Hilar cells that proliferate and produce new GCs could migrate to the GC layer, which has been proposed in the first 1–2 weeks of life (Namba et al. 2005). Alternatively, the hilar GCs that are produced may not migrate and if so, they would increase the number of hEGCs. The possibility that the hilus continues to be a site of proliferation throughout life is intriguing and some evidence for this has been published: Leung et al. 2012) showed that neurons can be produced in the hilus even in aged mice. Thus, the majority of adult-born GCs may be generated in the SGZ after PND30 and some may migrate to the hilus, but a small pool of GCs could emerge from the hilus and

remain there. The cells that divide in the hilus may be the vestiges of the tertiary matrix in early life.

F. Hilar Prox1-ir cells could be a subset of calretinin-ir "interneurons" of the hilus—Anatomical studies of rats have shown that a population of hilar cells exists in adult rodents that are calretinin-ir and co-express glutamate and glutamate decarboxylase 67 (GAD67), the synthetic enzyme for GABA (Soriano and Frotscher 1993; Martinez et al. 1999). The morphology of these cells is often like GCs because the soma shape and size are similar, and dendrites are spiny (Soriano and Frotscher 1993; Martinez et al. 1999). However, they are unlike GCs because the dendrites are multipolar or bipolar, and extend in many directions (Soriano and Frotscher 1993; Martinez et al. 1999). For this reason they have been considered to be interneurons. On the other hand, the multipolar/bipolar dendrites are like hEGCs studied in animal models of epilepsy (Scharfman et al. 2000; Pierce et al. 2011). Therefore, when a GC is present in the hilus, it appears to lose its polarity (i.e., dendrites to one side only). Thus, hilar calretinin-ir cells could be GCs. An argument is that the hilar calretinin-ir "interneurons" do not appear to have classic mossy fiber axons, i.e., they do not appear to have 'giant' boutons and a major portion of the axon in stratum lucidum. On the other hand, their axons are not always visible because of the preparation (Golgi or immunohistochemistry using antibodies to calretinin). In addition, immature GCs in the hilus that express calretinin may have immature GC axons without massive boutons or stratum lucidum projections (Namba et al. 2005). The fact that calretinin-ir 'interneurons' express glutamate as well as GAD67 argues that they are GC-like, because this has been shown for GCs in hippocampus but not other cell types (Sandler and Smith 1991; Munster-Wandowski et al. 2013). Thus, our data suggest that investigators should not assume that small calretinin-ir neurons in the hilus are interneurons. A subset of the calretinin-ir "interneurons" of the hilus could be immature GCs.

II. Deleting BAX in Nestin-expressing cells during the first postnatal week leads to an increase in hilar Prox1-ir cells

Removing *BAX* from Nestin-expressing precursors during the first postnatal week (i.e., PND2-P8) increased hilar Prox1-ir cell density in adulthood. The data are consistent with results from a constitutive *BAX* knockout (KO) mouse showing a robust population of hEGCs at adult ages (Sun et al. 2004; Myers et al. 2013).

We showed a subset of the Prox1-ir cells in the hilus of NCBax$^{f/f}$ mice expressed NeuN at PND60, similar to control mice. Thus, the percentages of Prox1-ir cells that co-expressed NeuN (Prox1+/NeuN− vs. Prox1+/NeuN+) were similar in both experimental and control groups. These data suggest that *BAX* regulates survival, not the degree of NeuN expression. This view is consistent with the data from Sun and colleagues, who showed no changes in proliferation, or the marker proliferating cell nuclear antigen (PCNA) in *BAX* KO mice (Sun et al. 2004).

III. Relevance to disease

In animal models and human temporal lobe epilepsy (TLE), hEGCs develop in the hilus (for reviews, see: Parent et al. 1997; Parent 2007; Scharfman and McCloskey 2009). The results

presented here are relevant to the mechanisms that lead to hEGCs. In the past, it has been suggested that hEGCs migrate from the SGZ into the hilus because somatostatin- and reelin-expressing hilar interneurons are killed in response to the insult or injury that induces epilepsy. With a loss of reelin in the hilus, SGZ cells more readily migrate to the hilus (Gong et al. 2007). It has also been suggested that hEGCs arise because seizures lead to altered $GABA_A$ receptors on hEGCs, so the normal effects of GABA as a regulator of migration are perturbed (Koyama et al. 2012). We previously proposed that genetic factors contribute to hEGC formation (Myers et al. 2013). The data provided here suggest that some hEGCs in animal models of TLE may be located in the hilus already, which has been discussed as a possibility before (Muramatsu et al. 2008).

Interestingly, the degree of Prox1+/NeuN+ coexpression at PND60 in the controls for tamoxifen-treated $NCBax^{f/f}$ mice (~90%; Figure 5E) was greater than normal PND60 C57BL/6J mice (~60%; Figure 2B). One would expect percentages to be comparable because they are normal mice of the same age. One explanation is that mouse strains were different — the $NCBax^{f/f}$ mice had a mixed C57BL6 and Sv129 background. If that is true, mouse strain plays an important role in the maturation of immature hilar GCs into mature hilar GCs. Another explanation is the stress of vehicle injections at PND2-8 somehow influenced the ultimate expression of NeuN, making more hilar Prox1-ir cells coexpress NeuN. In future studies it will be valuable to ask more about the regulation of hilar GCs and whether the degree these cells proliferate or become mature GCs can be manipulated. This is valuable because it could ultimately become an approach to repopulate the hilus with neurons after insults or injury damages hilar mossy cells and hilar interneurons.

IV. Summary

In summary, we have shown that a population of immature and mature GCs exists in the hilus of the C57BL/6 and SW mouse. This population varies depending on the age, site along the septotemporal axis, and strain. It is very large at PND16, especially in the septal DG. The numbers of hilar Prox1-ir cells can be increased by deleting *BAX* from Nestin-expressing cells in the first week of life. There are increased numbers of hilar Prox1-ir cells in these animals, and most of them develop NeuN expression by PND60, suggesting that the proportion of cells which become mature neurons remains high.

Supplementary Material

Refer to Web version on PubMed Central for supplementary material.

Acknowledgments

Supported by NIH MH-090606, NS-081203 and the New York State Office of Mental Health.

References

Altman J, Das GD. Autoradiographic and histological evidence of postnatal hippocampal neurogenesis in rats. J Comp Neurol. 1965; 124:319–335. [PubMed: 5861717]

Altman J, Bayer SA. Mosaic organization of the hippocampal neuroepithelium and the multiple germinal sources of dentate granule cells. J Comp Neurol. 1990a; 301:325–342. [PubMed: 2262594]

Altman J, Bayer SA. Migration and distribution of two populations of hippocampal granule cell precursors during the perinatal and postnatal periods. J Comp Neurol. 1990b; 301:365–381. [PubMed: 2262596]

Amaral DG. A golgi study of cell types in the hilar region of the hippocampus in the rat. J Comp Neurol. 1978; 182:851–914. [PubMed: 730852]

Amaral DG, Dent JA. Development of the mossy fibers of the dentate gyrus: I. A light and electron microscopic study of the mossy fibers and their expansions. J Comp Neurol. 1981; 195:51–86. [PubMed: 7204652]

Attardo A, Fabel K, Krebs J, Haubensak W, Huttner WB, Kempermann G. Tis21 expression marks not only populations of neurogenic precursor cells but also new postmitotic neurons in adult hippocampal neurogenesis. Cereb Cortex. 2010; 20:304–314. [PubMed: 19482889]

Bayer SA. Changes in the total number of dentate granule cells in juvenile and adult rats: A correlated volumetric and 3h-thymidine autoradiographic study. Exp Brain Res. 1982; 46:315–323. [PubMed: 7095040]

Bayer SA, Yackel JW, Puri PS. Neurons in the rat dentate gyrus granular layer substantially increase during juvenile and adult life. Science. 1982; 216:890–892. [PubMed: 7079742]

Brandt MD, Jessberger S, Steiner B, Kronenberg G, Reuter K, Bick-Sander A, von der Behrens W, Kempermann G. Transient calretinin expression defines early postmitotic step of neuronal differentiation in adult hippocampal neurogenesis of mice. Mol Cell Neurosci. 2003; 24:603–613. [PubMed: 14664811]

Brown JP, Couillard-Despres S, Cooper-Kuhn CM, Winkler J, Aigner L, Kuhn HG. Transient expression of doublecortin during adult neurogenesis. J Comp Neurol. 2003; 467:1–10. [PubMed: 14574675]

Choi YS, Cho KO, Kim SY. Asymmetry in enhanced neurogenesis in the rostral dentate gyrus following kainic acid-induced status epilepticus in adult rats. Arch Pharm Res. 2007; 30:646–652. [PubMed: 17615686]

Cowan WM, Stanfield BB, Kishi K. The development of the dentate gyrus. Current topics in developmental biology. 1980; 15(Pt 1):103–157. [PubMed: 6778660]

Cowen DS, Takase LF, Fornal CA, Jacobs BL. Age-dependent decline in hippocampal neurogenesis is not altered by chronic treatment with fluoxetine. Brain Res. 2008; 1228:14–19. [PubMed: 18616933]

Cushman JD, Maldonado J, Kwon EE, Garcia AD, Fan G, Imura T, Sofroniew MV, Fanselow MS. Juvenile neurogenesis makes essential contributions to adult brain structure and plays a sex-dependent role in fear memories. Front Behav Neurosci. 2012; 6:3. [PubMed: 22347173]

Dayer AG, Ford AA, Cleaver KM, Yassaee M, Cameron HA. Short-term and long-term survival of new neurons in the rat dentate gyrus. J Comp Neurol. 2003; 460:563–572. [PubMed: 12717714]

Farrar CE, Huang CS, Clarke SG, Houser CR. Increased cell proliferation and granule cell number in the dentate gyrus of protein repair-deficient mice. J Comp Neurol. 2005; 493:524–537. [PubMed: 16304629]

Faulkner RL, Jang MH, Liu XB, Duan X, Sailor KA, Kim JY, Ge S, Jones EG, Ming GL, Song H, Cheng HJ. Development of hippocampal mossy fiber synaptic outputs by new neurons in the adult brain. Proc Natl Acad Sci U S A. 2008; 105:14157–14162. [PubMed: 18780780]

Ferland RJ, Gross RA, Applegate CD. Differences in hippocampal mitotic activity within the dorsal and ventral hippocampus following flurothyl seizures in mice. Neurosci Lett. 2002; 332:131–135. [PubMed: 12384228]

Gage, FH., G, K., H, S. Neurogenesis. Cold spring Harbor: Cold Spring Harbor Press; 2015.

Galeeva A, Treuter E, Tomarev S, Pelto-Huikko M. A prospero-related homeobox gene prox-1 is expressed during postnatal brain development as well as in the adult rodent brain. Neuroscience. 2007; 146:604–616. [PubMed: 17368742]

Galichet C, Guillemot F, Parras CM. Neurogenin 2 has an essential role in development of the dentate gyrus. Development. 2008; 135:2031–2041. [PubMed: 18448566]

Gerdes J, Li L, Schlueter C, Duchrow M, Wohlenberg C, Gerlach C, Stahmer I, Kloth S, Brandt E, Flad HD. Immunobiochemical and molecular biologic characterization of the cell proliferation-associated nuclear antigen that is defined by monoclonal antibody ki-67. Am J Pathol. 1991; 138:867–873. [PubMed: 2012175]

Gong C, Wang TW, Huang HS, Parent JM. Reelin regulates neuronal progenitor migration in intact and epileptic hippocampus. J Neurosci. 2007; 27:1803–1811. [PubMed: 17314278]

Gould E, Woolley CS, McEwen BS. Naturally occurring cell death in the developing dentate gyrus of the rat. J Comp Neurol. 1991; 304:408–418. [PubMed: 2022756]

Hayes NL, Nowakowski RS. Dynamics of cell proliferation in the adult dentate gyrus of two inbred strains of mice. Brain research Developmental brain research. 2002; 134:77–85. [PubMed: 11947938]

He J, Crews FT. Neurogenesis decreases during brain maturation from adolescence to adulthood. Pharmacol Biochem Behav. 2007; 86:327–333. [PubMed: 17169417]

Heine VM, Maslam S, Joels M, Lucassen PJ. Prominent decline of newborn cell proliferation, differentiation, and apoptosis in the aging dentate gyrus, in absence of an age-related hypothalamus-pituitary-adrenal axis activation. Neurobiol Aging. 2004; 25:361–375. [PubMed: 15123342]

Ho A, Villacis AJ, Svirsky SE, Foilb AR, Romeo RD. The pubertal-related decline in cellular proliferation and neurogenesis in the dentate gyrus of male rats is independent of the pubertal rise in gonadal hormones. Dev Neurobiol. 2012; 72:743–752. [PubMed: 21990242]

Iwano T, Masuda A, Kiyonari H, Enomoto H, Matsuzaki F. Prox1 postmitotically defines dentate gyrus cells by specifying granule cell identity over CA3 pyramidal cell fate in the hippocampus. Development. 2012; 139:3051–3062. [PubMed: 22791897]

Jinno S. Topographic differences in adult neurogenesis in the mouse hippocampus: A stereology-based study using endogenous markers. Hippocampus. 2011a; 21:467–480. [PubMed: 20087889]

Jinno S. Decline in adult neurogenesis during aging follows a topographic pattern in the mouse hippocampus. J Comp Neurol. 2011b; 519:451–466. [PubMed: 21192078]

Kempermann G, Kuhn HG, Gage FH. Genetic influence on neurogenesis in the dentate gyrus of adult mice. Proc Natl Acad Sci U S A. 1997; 94:10409–10414. [PubMed: 9294224]

Kempermann G, Jessberger S, Steiner B, Kronenberg G. Milestones of neuronal development in the adult hippocampus. Trends Neurosci. 2004; 27:447–452. [PubMed: 15271491]

Key G, Meggetto F, Becker MH, al Saati T, Schluter C, Duchrow M, Delsol G, Gerdes J. Immunobiochemical characterization of the antigen detected by monoclonal antibody ind.64. Evidence that ind.64 reacts with the cell proliferation associated nuclear antigen previously defined by ki-67. Virchows Archiv B, Cell pathology including molecular pathology. 1992; 62:259–262. [PubMed: 1279888]

Key G, Becker MH, Baron B, Duchrow M, Schluter C, Flad HD, Gerdes J. New ki-67-equivalent murine monoclonal antibodies (mib 1–3) generated against bacterially expressed parts of the ki-67 cdna containing three 62 base pair repetitive elements encoding for the ki-67 epitope. Lab Invest. 1993; 68:629–636. [PubMed: 7685843]

Kim JS, Jung J, Lee HJ, Kim JC, Wang H, Kim SH, Shin T, Moon C. Differences in immunoreactivities of ki-67 and doublecortin in the adult hippocampus in three strains of mice. Acta Histochem. 2009; 111:150–156. [PubMed: 18649926]

Koyama R, Tao K, Sasaki T, Ichikawa J, Miyamoto D, Muramatsu R, Matsuki N, Ikegaya Y. GABAergic excitation after febrile seizures induces ectopic granule cells and adult epilepsy. Nat Med. 2012; 18:1271–1278. [PubMed: 22797810]

Lavado A, Lagutin OV, Chow LM, Baker SJ, Oliver G. Prox1 is required for granule cell maturation and intermediate progenitor maintenance during brain neurogenesis. PLoS Biol. 2010; 8

Lazarov O, Mattson MP, Peterson DA, Pimplikar SW, van Praag H. When neurogenesis encounters aging and disease. Trends Neurosci. 2010; 33:569–579. [PubMed: 20961627]

Leung L, Andrews-Zwilling Y, Yoon SY, Jain S, Ring K, Dai J, Wang MM, Tong L, Walker D, Huang Y. Apolipoprotein e4 causes age- and sex-dependent impairments of hilar GABAergic interneurons and learning and memory deficits in mice. PloS one. 2012; 7:e53569. [PubMed: 23300939]

Li G, Pleasure SJ. Genetic regulation of dentate gyrus morphogenesis. Prog Brain Res. 2007; 163:143–152. [PubMed: 17765716]

Li G, Kataoka H, Coughlin SR, Pleasure SJ. Identification of a transient subpial neurogenic zone in the developing dentate gyrus and its regulation by cxcl12 and reelin signaling. Development. 2009; 136:327–335. [PubMed: 19103804]

Marti-Subirana A, Soriano E, Garcia-Verdugo JM. Morphological aspects of the ectopic granule-like cellular populations in the albino rat hippocampal formation: A golgi study. J Anat. 1986; 144:31–47. [PubMed: 2447048]

Martin LA, Tan SS, Goldowitz D. Clonal architecture of the mouse hippocampus. J Neurosci. 2002; 22:3520–3530. [PubMed: 11978829]

Martinez A, Ruiz M, Soriano E. Spiny calretinin-immunoreactive neurons in the hilus and CA3 region of the rat hippocampus: Local axon circuits, synaptic connections, and glutamic acid decarboxylase 65/67 mrna expression. J Comp Neurol. 1999; 404:438–448. [PubMed: 9987989]

Mathews EA, Morgenstern NA, Piatti VC, Zhao C, Jessberger S, Schinder AF, Gage FH. A distinctive layering pattern of mouse dentate granule cells is generated by developmental and adult neurogenesis. J Comp Neurol. 2010; 518:4479–4490. [PubMed: 20886617]

McCloskey DP, Hintz TM, Pierce JP, Scharfman HE. Stereological methods reveal the robust size and stability of ectopic hilar granule cells after pilocarpine-induced status epilepticus in the adult rat. Eur J Neurosci. 2006; 24:2203–2210. [PubMed: 17042797]

Mullen RJ, Buck CR, Smith AM. Neun, a neuronal specific nuclear protein in vertebrates. Development. 1992; 116:201–211. [PubMed: 1483388]

Munster-Wandowski A, Gomez-Lira G, Gutierrez R. Mixed neurotransmission in the hippocampal mossy fibers. Frontiers in cellular neuroscience. 2013; 7:210. [PubMed: 24319410]

Muramatsu R, Ikegaya Y, Matsuki N, Koyama R. Early-life status epilepticus induces ectopic granule cells in adult mice dentate gyrus. Exp Neurol. 2008; 211:503–510. [PubMed: 18420198]

Myers CE, Bermudez-Hernandez K, Scharfman HE. The influence of ectopic migration of granule cells into the hilus on dentate gyrus-CA3 function. PloS one. 2013; 8:e68208. [PubMed: 23840835]

Namba T, Mochizuki H, Onodera M, Mizuno Y, Namiki H, Seki T. The fate of neural progenitor cells expressing astrocytic and radial glial markers in the postnatal rat dentate gyrus. Eur J Neurosci. 2005; 22:1928–1941. [PubMed: 16262632]

Nicola Z, Fabel K, Kempermann G. Development of the adult neurogenic niche in the hippocampus of mice. Frontiers in neuroanatomy. 2015; 9:53. [PubMed: 25999820]

Oliver G, Sosa-Pineda B, Geisendorf S, Spana EP, Doe CQ, Gruss P. Prox 1, a prospero-related homeobox gene expressed during mouse development. Mech Dev. 1993; 44:3–16. [PubMed: 7908825]

Parent JM, Yu TW, Leibowitz RT, Geschwind DH, Sloviter RS, Lowenstein DH. Dentate granule cell neurogenesis is increased by seizures and contributes to aberrant network reorganization in the adult rat hippocampus. J Neurosci. 1997; 17:3727–3738. [PubMed: 9133393]

Parent JM. Adult neurogenesis in the intact and epileptic dentate gyrus. Prog Brain Res. 2007; 163:529–540. [PubMed: 17765736]

Paxinos, G., Watson, C. The rat brain in stereotaxic coordinates. Academic Press; 2007.

Pierce JP, McCloskey DP, Scharfman HE. Morphometry of hilar ectopic granule cells in the rat. J Comp Neurol. 2011; 519:1196–1218. [PubMed: 21344409]

Pleasure SJ, Collins AE, Lowenstein DH. Unique expression patterns of cell fate molecules delineate sequential stages of dentate gyrus development. J Neurosci. 2000; 20:6095–6105. [PubMed: 10934259]

Pritchett, KR., Taft, RA. Chapter 3 — reproductive biology of the laboratory mouse. In: Fox, JG.Davisson, MT.Quimby, FW.Barthold, SW.Newcomer, CE., Smith, AL., editors. The mouse in biomedical research. second. Burlington: Academic Press; 2007. p. 91-121.

Rao MS, Hattiangady B, Shetty AK. The window and mechanisms of major age-related decline in the production of new neurons within the dentate gyrus of the hippocampus. Aging cell. 2006; 5:545–558. [PubMed: 17129216]

Sahay A, Scobie KN, Hill AS, O'Carroll CM, Kheirbek MA, Burghardt NS, Fenton AA, Dranovsky A, Hen R. Increasing adult hippocampal neurogenesis is sufficient to improve pattern separation. Nature. 2011; 472:466–470. [PubMed: 21460835]

Sandler R, Smith AD. Coexistence of GABA and glutamate in mossy fiber terminals of the primate hippocampus: An ultrastructural study. J Comp Neurol. 1991; 303:177–192. [PubMed: 1672874]

Scharfman H, Goodman J, McCloskey D. Ectopic granule cells of the rat dentate gyrus. Dev Neurosci. 2007; 29:14–27. [PubMed: 17148946]

Scharfman HE, Goodman JH, Sollas AL. Granule-like neurons at the hilar/CA3 border after status epilepticus and their synchrony with area CA3 pyramidal cells: Functional implications of seizure-induced neurogenesis. J Neurosci. 2000; 20:6144–6158. [PubMed: 10934264]

Scharfman HE, Sollas AE, Berger RE, Goodman JH, Pierce JP. Perforant path activation of ectopic granule cells that are born after pilocarpine-induced seizures. Neuroscience. 2003; 121:1017–1029. [PubMed: 14580952]

Scharfman HE, McCloskey DP. Postnatal neurogenesis as a therapeutic target in temporal lobe epilepsy. Epilepsy Res. 2009; 85:150–161. [PubMed: 19369038]

Schauwecker PE. Genetic influence on neurogenesis in the dentate gyrus of two strains of adult mice. Brain Res. 2006; 1120:83–92. [PubMed: 16999941]

Schlessinger AR, Cowan WM, Gottlieb DI. An autoradiographic study of the time of origin and the pattern of granule cell migration in the dentate gyrus of the rat. J Comp Neurol. 1975; 159:149–175. [PubMed: 1112911]

Seki T, Arai Y. Age-related production of new granule cells in the adult dentate gyrus. Neuroreport. 1995; 6:2479–2482. [PubMed: 8741746]

Snyder JS, Radik R, Wojtowicz JM, Cameron HA. Anatomical gradients of adult neurogenesis and activity: Young neurons in the ventral dentate gyrus are activated by water maze training. Hippocampus. 2009; 19:360–370. [PubMed: 19004012]

Soriano E, Frotscher M. Spiny nonpyramidal neurons in the CA3 region of the rat hippocampus are glutamate-like immunoreactive and receive convergent mossy fiber input. J Comp Neurol. 1993; 333:435–448. [PubMed: 8102385]

Steiner B, Zurborg S, Horster H, Fabel K, Kempermann G. Differential 24 h responsiveness of prox1-expressing precursor cells in adult hippocampal neurogenesis to physical activity, environmental enrichment, and kainic acid-induced seizures. Neuroscience. 2008; 154:521–529. [PubMed: 18502050]

Sun W, Winseck A, Vinsant S, Park OH, Kim H, Oppenheim RW. Programmed cell death of adult-generated hippocampal neurons is mediated by the proapoptotic gene bax. J Neurosci. 2004; 24:11205–11213. [PubMed: 15590937]

Szabadics J, Varga C, Brunner J, Chen K, Soltesz I. Granule cells in the CA3 area. J Neurosci. 2010; 30:8296–8307. [PubMed: 20554881]

Urban N, Guillemot F. Neurogenesis in the embryonic and adult brain: Same regulators, different roles. Frontiers in cellular neuroscience. 2014; 8:396. [PubMed: 25505873]

Volz F, Bock HH, Gierthmuehlen M, Zentner J, Haas CA, Freiman TM. Stereologic estimation of hippocampal GluR2/3- and calretinin-immunoreactive hilar neurons (presumptive mossy cells) in two mouse models of temporal lobe epilepsy. Epilepsia. 2011; 52:1579–1589. [PubMed: 21635231]

von Bohlen Und Halbach O. Immunohistological markers for staging neurogenesis in adult hippocampus. Cell Tissue Res. 2007; 329:409–420. [PubMed: 17541643]

Zhang J, Jiao J. Molecular biomarkers for embryonic and adult neural stem cell and neurogenesis. Biomed Res Int. 2015; 2015:727542. [PubMed: 26421301]

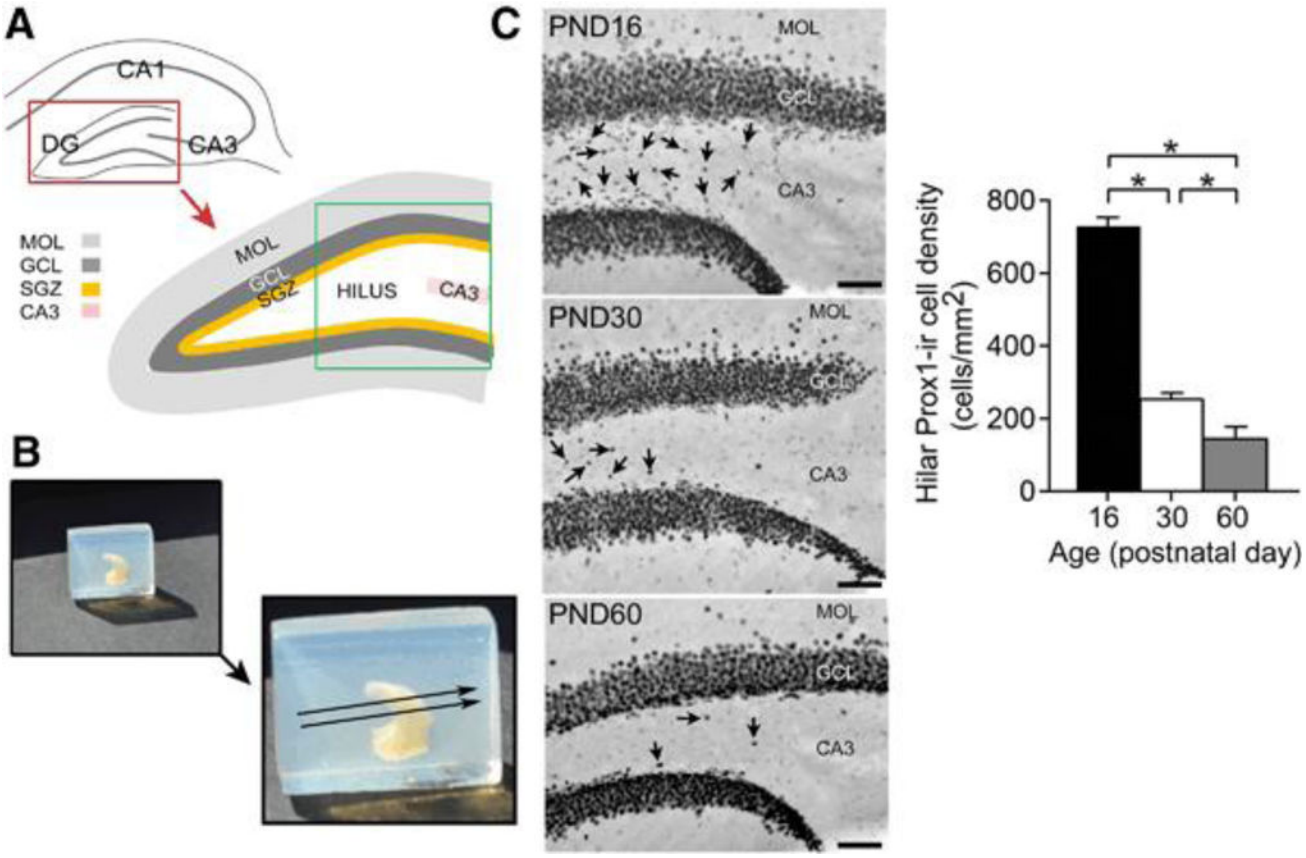

Figure 1. Hilar Prox1-ir cells are robust in C57BL/6J mice at PND16 and decline with age

A. A diagram of the septal hippocampus in a section transverse to the longitudinal axis of the hippocampus. DG = dentate gyrus; GCL = granule cell layer; SGZ = subgranular zone; MOL = molecular layer; CA3 = CA3 pyramidal cell layer. The area outlined by the green box is shown in C.

B. The method to make transverse sections of an entire hippocampus isolated from one hemisphere (referred to as the isolated hippocampus in the text) is shown. Top left: One hippocampus in a block of agar, before gluing it to a vibratome stage for sectioning. Bottom right: The direction of sectioning, transverse to the long axis of the hippocampus, is shown by the arrows.

C. Prox1-ir in a section from an isolated hippocampus shows the large numbers of hilar Prox1-ir cells in a PND16 mouse (Top), fewer hilar Prox1-ir cells in a PND30 mouse (Center), and the least in a PND60 mouse (Bottom). Arrows point to hilar Prox1-ir cells. Calibration = 75 μm.

D. Mean hilar Prox1-ir cell density of PND16 (n = 4); PND30 (n = 5), and PND60 mice (n = 5) estimated from isolated hippocampi. A one-way ANOVA showed a significant effect of age [$F(2, 11)$ 351.20; $p < 0.0001$] with PND16 mice exhibiting more Prox1-ir cells in the hilar region compared to PND30, and more Prox1-ir cells at PND30 compared to PND60 (post-hoc tests, $p < 0.05$ indicated by asterisks). Supplemental Figure 1 provides the cell numbers and volume calculations used to establish density.

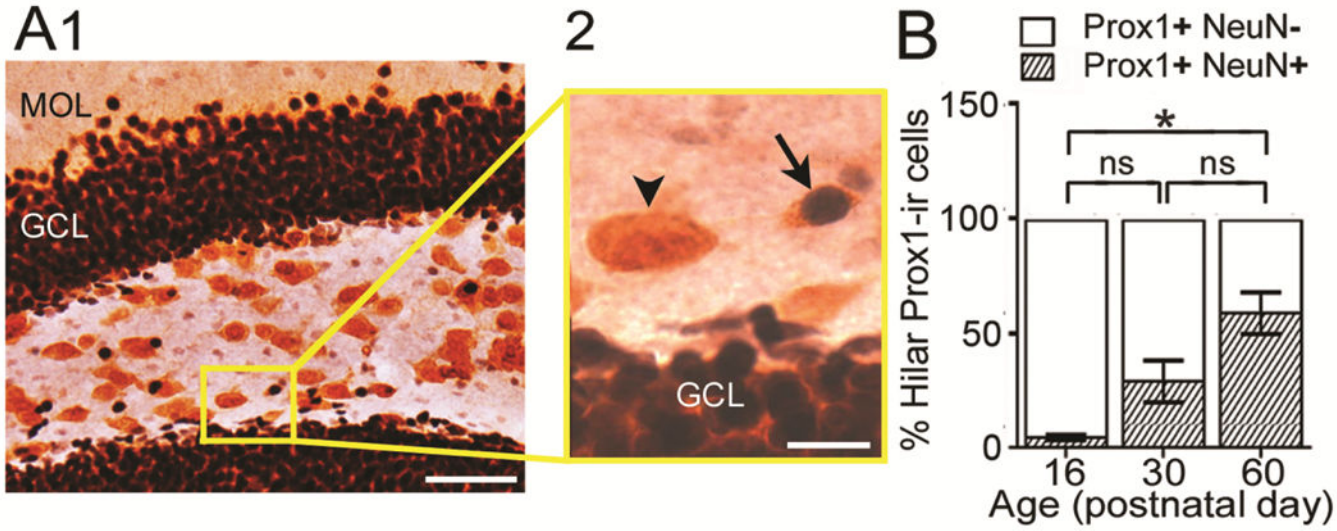

Figure 2. The subset of hilar Prox1-ir cells in C57BL/6J mice that co-expressed NeuN increase with age

A. Example of Prox1-ir and NeuN-ir double-labeling.

1. Low power. The boxed area is shown at higher power in A2. MOL = molecular layer; GCL = granule cell layer. Calibration = 50 μm.

2. The arrow points to a double-labeled cell with a dark Prox1 nucleus surrounded by NeuN-stained cytoplasm (diffuse orange staining, corresponding to NovaRed as described in the Methods). The arrowhead points to a Prox1-ir cell that was not double-labeled with NeuN. Calibration = 10 μm.

B. Percentage of Prox1-ir cells that did (shaded bars) or did not (white bars) co-express NeuN at PND16, 30 and 60 (n = 3/group). A one-way ANOVA was significant [$F(2, 6) 15.52$; $p = 0.04$]. There was a significant difference between PND16 and PND60, with PND16 showing fewer double-labeled cells (post-hoc tests, $p < 0.05$). PND30 mice did not significantly differ from PND16 or PND60 mice (post-hoc tests, $p > 0.05$). ns = not significant.

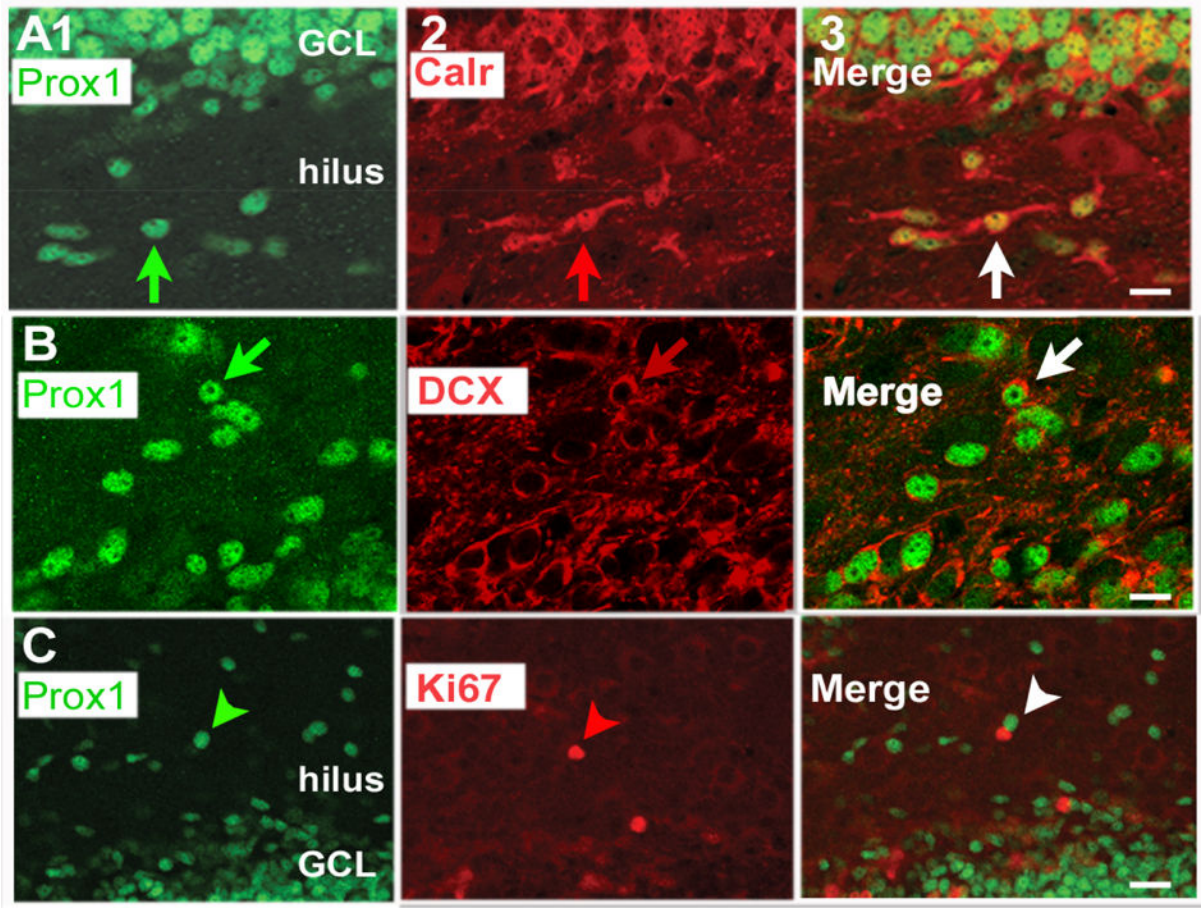

Figure 3. Most hilar Prox1-ir cells at PND16 in C57BL/6J mice co-express calretinin or DCX but not Ki67

A. 1. Prox1 (green) staining in a section from a PND16 mouse.

2. The same section, showing calretinin (red) staining.

3. The merged image shows cells that are double-labeled in yellow (white arrow). GCL = granule cell layer. Calibration in A3 = 15 μm. Additional images are shown in Supplemental Figure 4 and Supplemental Movie 1.

B. 1. Prox1 (green) staining in a section from a PND16 mouse.

2. The same section, showing DCX (red) staining.

3. The merged image shows cells that are double-labeled have a green center reflecting the nuclear Prox1 stain and red processes reflecting DCX expression (white arrow). In some cases DCX is expressed in the cytoplasm (red arrow in B2). Calibration in B3 = 10 μm. Additional images are shown in Supplemental Figure 5.

C. 1. Prox1 (green) staining in a section from a PND16 mouse.

2. The same section, showing Ki67 (red) staining.

3. The merged image shows cells that are green or red (arrowhead) but no evidence of cells that are double-labeled. Calibration in C3 = 20 μm.

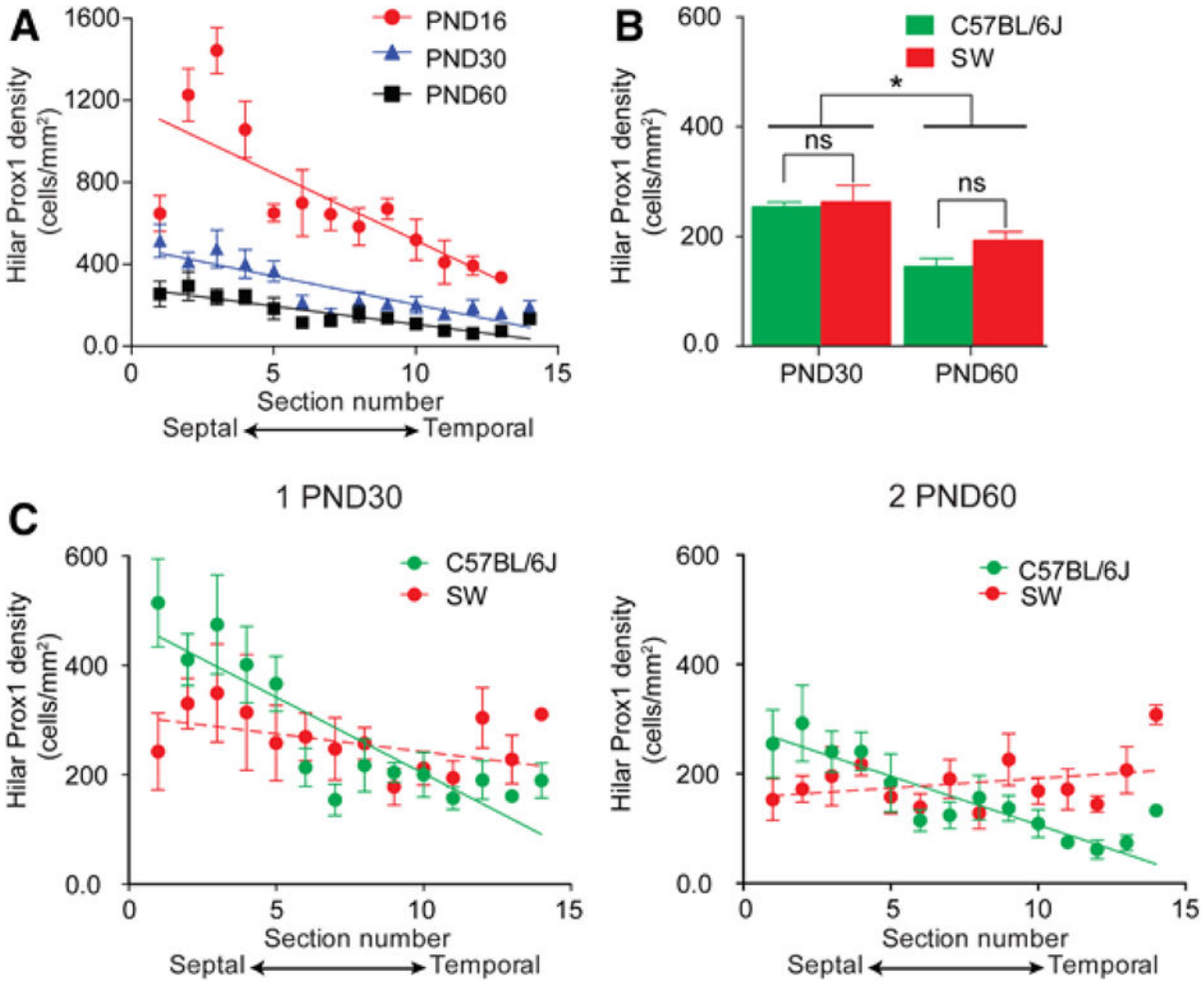

Figure 4. Hilar Prox1-ir cell density varies across the septotemporal axis in C57BL/6J but not SW mice

A. Mean hilar Prox1-ir cell density in 4 C57BL/6J mice at PND16 (red circles), 5 C57BL/6J at PND30 (blue triangles) and 5 C57BL/6J at PND60 (black squares). There was a significant linear relationship between hilar Prox1-ir cell density and the section location for the three ages (linear regression; PND16: $p < 0.0001$; PND30: $p < 0.0001$; PND60: $p < 0.0001$). Slopes were significantly different (ANCOVA; PND16: −65.5 ± 11.3; PND30: −27.8 ± 3.7; PND60: −17.9 ± 2.7; $p < 0.0001$).

To determine if differences were significant by a two-way RMANOVA, sample size was 4/group because one animal at PND30 and one animal at PND60 had one section that was damaged during the sectioning/processing. The RMANOVA showed a significant effect of age [$F(2, 9)$ 180.60; $p < 0.0001$] and septotemporal level [$F(11, 99)$ 15.76; $p < 0.0001$] with a significant interaction between factors [$F(22, 99)$ 4.38; $p < 0.001$], consistent with a steeper slope in PND16 data compared to older ages.

B. Hilar Prox1-ir cell density in C57BL/6J and SW mice at PND30 and PND60 ($n = 5$/group). There was no effect of strain on hilar Prox1-ir cell density by two-way ANOVA [$F(1, 16)$ 2.13; $p = 0.164$] but there was an effect of age [$F(1, 16)$ 21.42; $p = 0.0003$], with

PND30 mice exhibiting significantly greater hilar Prox1-ir cell density in both C57BL/6J and SW mice (post-hoc tests, $p < 0.05$).

C. 1. Hilar Prox1-ir cell density for individual sections of PND30 C57BL/6J and SW mice (n = 5/group). C57BL/6J mice showed a significant linear relationship between hilar Prox1-ir density and section location for each age (Linear regression; $p < 0.0001$) but SW mice did not ($p > 0.05$).

2. Hilar Prox1-ir cell density for PND60 C57BL/6J and SW mice (n = 5/group).C57BL/6J mice showed a significant linear relationship between hilar Prox1-ir density and section level (Linear regression; $p < 0.0001$) but SW mice did not.

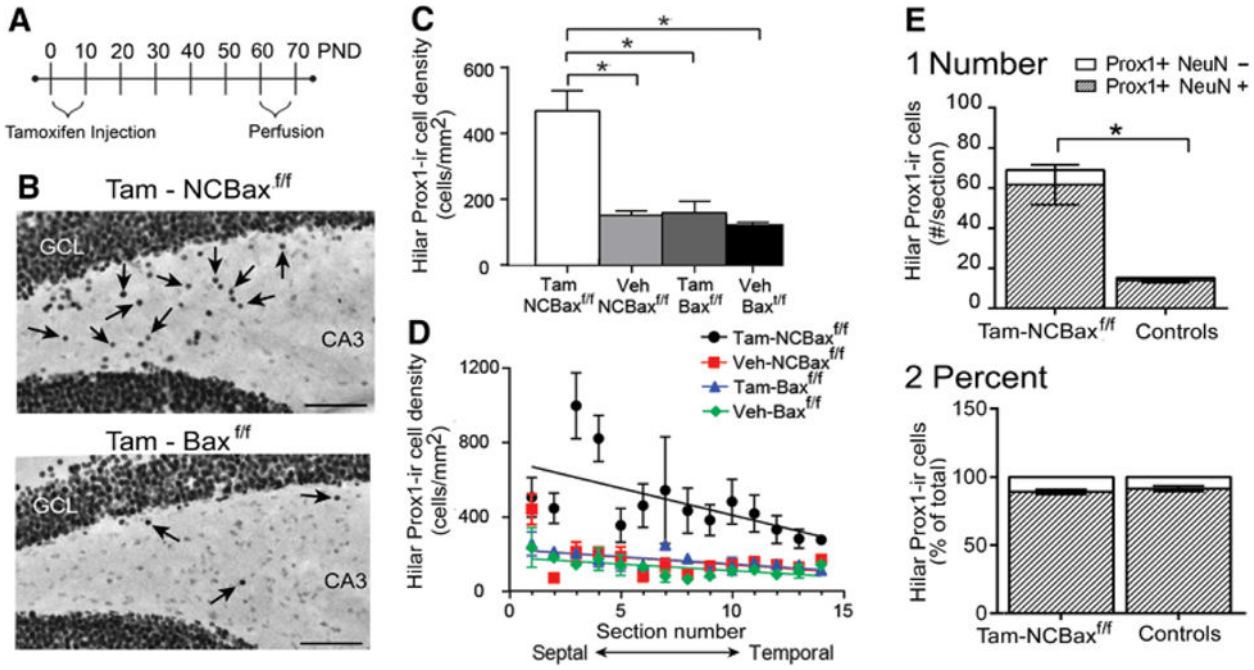

Figure 5. Selective deletion of *BAX* in Nestin-expressing cells increases hilar Prox1-ir cell density

A. A schematic illustrates the experimental timeline for tamoxifen injections (daily, PND2-8) and perfusions (PND63-66).

B. An example of Prox1-ir for a section in a tamoxifen-treated NCBax$^{f/f}$ mouse where there are numerous hilar Prox1-ir cells (Top, arrows) vs. a section from a tamoxifen-treated Bax$^{f/f}$ mouse where there are few Prox1-ir cells (Bottom). Sections are from a similar septotemporal level. GCL = granule cell layer. Calibration = 75 μm.

C. One-way ANOVA showed that tamoxifen-treated NCBax$^{f/f}$ mice had significantly greater hilar Prox1-ir cell density compared to all other groups [one way-ANOVA; F (3, 8) 23.50; p = 0.0003 followed by post-hoc tests, $p < 0.05$; asterisks]. Veh = vehicle.

D. Hilar Prox1-ir cell density is plotted along the septotemporal axis.

E. The number of Prox1-ir cells that were double-labeled with NeuN (shaded), and the number of Prox1-ir cells without NeuN co-expression (white) are shown for tamoxifen-treated NCBax$^{f/f}$ mice (n=3) and vehicle-treated mice (NCBax$^{f/f}$ and Bax$^{f/f}$, mice, pooled, n = 3).

1. Tamoxifen-treated mice had more double-labeled cells than vehicle-treated mice (Student's t-test, p = 0.009).

The percentage of double-labeled cells did not significantly differ (Student's t-test, p = 0.431).